Proceedings of the
Annual Stability Conference
Structural Stability Research Council
Atlanta, Georgia, April 21-24, 2026

Consideration of modified slenderness ratio for joist girder top chord buckling

Kubilay Cicek[1], Useok Kim[2], Hannah B. Blum[3]

Abstract

Open-web steel joists are widely used in floor and roof systems due to their light weight, ease of fabrication, and efficient load-carrying behavior. However, certain failure modes, particularly top chord buckling, can govern design, especially in long-span joists or systems with limited lateral bracing. Previous studies have examined the effects of lateral support length, material properties, and filler placement on top chord buckling and suggested the use of reduced effective length factors.

This study focuses on slenderness-related behavior of steel joist girders, intentionally considering top chord buckling as the governing failure mode. Three different joist girder layouts were developed, each using four cross-section sizes and two lateral support lengths. Slenderness ratios were calculated using both the standard Steel Joist Institute (SJI) equation and the modified version provided in the SJI standard. These values were used to determine expected buckling type (elastic or inelastic) and to calculate the corresponding critical buckling stress, F_{cr}, per SJI specifications.

Finite element models were developed using MASTAN2. Additional analyses were performed using both basic and advanced section modeling to investigate the effect of least radius of gyration r_z, and fillers were introduced to examine the influence of l_s. After determining top chord buckling loads, the axial forces in the top chord at buckling were used to calculate F_{cr} and effective slenderness ratios, which were compared to Specification values.

Results showed that both the standard and modified slenderness formulas overestimated slenderness ratios compared to slenderness ratios back-calculated from MASTAN2 buckling analysis results. Similarly, F_{cr} values from finite element analysis indicated greater capacities than SJI predictions, suggesting the modified formula may be overly conservative.

1. Introduction

Steel joist girders are commonly used in commercial buildings due to their efficiency and cost-effectiveness. Traditionally, the design of joist girder chord members has relied on conservative

[1]PhD Candidate, University of Wisconsin-Madison, <cicek@wisc.edu>
[2]PhD Student, University of Wisconsin-Madison, <useok.kim@wisc.edu>
[3]Alain H. Peyrot Associate Professor, University of Wisconsin-Madison, <hannah.blum@wisc.edu>

assumptions, specifically an effective length factor (k) of 0.94 (Steel Joist Institute, 2020). While this ensures safety, it often leads to over-designed structures because it may not fully account for the partial restraint provided by the web members where they attach to the chords, nor for the impact of fillers between the chord angles.

A recent study (Cicek, Sputo, and Blum, 2024) aimed to improve k-factor estimates of joist chord members by considering several critical variables. These include web member stiffness, filler locations, geometric imperfections, material property variations, and lateral bracing conditions. The goal of this research was to more accurately capture real buckling behavior and encourage more efficient material use. In a related prior study (Kim, Sputo, and Blum, 2024), the applicability of a modified slenderness approach—originally developed for built-up web members—to joist chord members in compression was investigated. That study focused on bottom chord buckling under uplift loading and evaluated the influence of least radius of gyration (r_z) and filler spacing (l_s) using detailed finite element analyses in MASTAN2. The results indicated that neither the current SJI chord slenderness formulation nor the proposed modified slenderness approach are recommended for joist chord members. This was attributed to the fact that both formulations idealize the compression chord as being under uniform axial compression, without explicitly accounting for the elastic restraint provided by attached web members. These findings highlighted the need for further investigation into more representative effective length formulations for joist chord buckling.

Building on this motivation, the present study investigates whether the modified slenderness ratio—which accounts for the least radius of gyration (r_z) and the distance between fillers and panel points (l_s)—is necessary for compression chord design for joist girders. Three joist girder layouts provided by the Steel Joist Institute (SJI) were used, each featuring four different cross-sections. These configurations were modeled in MASTAN2 using 3D finite element analysis to perform both elastic and inelastic eigenvalue buckling simulations.

The resulting buckling capacities were then used to calculate the resulting slenderness ratios and critical stresses (F_{cr}) using the equations in the AISC and SJI design standards (AISC 360-10, 2010, Steel Joist Institute, 2020). This methodology allows for a direct comparison between the simulated structural behavior and the theoretical formulas used in practice.

Ultimately, this paper evaluates the individual and combined effects of r_z and l_s on the actual slenderness ratios and critical stress values of the top chord joist girder members to determine if current modified slenderness requirements are appropriate. The findings aim to clarify the conditions under which these modifications can be essential for safety versus if they may lead to unnecessary design complexity. The following sections detail the modeling approach, the slenderness calculation process, and a comprehensive discussion of the results. Additional details can be found in a technical report (Kim, Cicek, and Blum, 2025).

2. Designs and Finite Element Modeling

SJI member companies designed three joist girders with varying layouts subjected to gravity loads to identify conditions under which the modified slenderness ratio becomes critical. Each layout includes members with various cross-sectional sizes, and to assess the influence of lateral support length on top chord performance, two different lateral support configurations were applied to each

model.

The modified slenderness ratio, as defined in the SJI 100-2020 Standard (Steel Joist Institute, 2020), is given in Eq. 1:

$$\left(\frac{k\ell}{r_y}\right)_m = \sqrt{\left(\frac{k\ell}{r_y}\right)^2 + \left(\frac{k_i \ell_s}{r_z}\right)^2} \tag{1}$$

where *k* is the effective length factor; *l* is the center-to-center length between panel points; r_y is the radius of gyration about the vertical axis of joist girder cross section; l_s is the maximum spacing between a panel point and a filler (tie), or between adjacent fillers; and r_z is the least radius of gyration of a member component. k_i was used as 0.5 for this study since the chords were designed as back-to-back double angles.

To better understand the effects of the modified slenderness ratio, additional analyses were conducted by focusing on its key parameters, the least radius of gyration (r_z) and the unbraced length between top chord members (l_s)—represented by modeling filler elements—were examined to see their individual impacts on the results.

A total of 96 Finite Element Models were analyzed for buckling by combining three girder designs (namely SJI1, SJI2 and SJI3), four different chord member cross-sections (coded from A to D, eg. SJI1A, with section size and thickness increasing from A to D), and two unbraced lengths. Additionally, two modeling options each for r_z and l_s were considered, resulting in $3 \times 4 \times 2 \times 2 \times 2 = 96$ distinct configurations.

2.1 Finite Element Modeling

The SJI girder designs were designed to have top chord buckling failure. Hence eigenvalue analyses were completed to capture the buckling behavior of each model in MASTAN2 and the required axial forces obtained from the analysis were used to calculate the resulting slenderness ratio and corresponding critical stress (F_{cr}). Additionally, ABAQUS models were developed to verify the modeling approach used in MASTAN2 through second-order inelastic analysis.

In MASTAN2, beam elements were used for all members, with rigid fillers placed at web-to-chord connection points. Each single angle of the back-to-back angles comprising the top and bottom chords were modeled as a separate section, and connected through fillers at panel points and at predefined locations of fillers shown in Fig. 1. Cross-sections were modeled using MSASect, assuming an elastic-perfectly-plastic material ($E = 29,000$ ksi, and $F_y = 50$ ksi). To ensure numerical stability, web member end moments were assigned a semi-rigid release of 0.001 (Sippel et al., 2020), and warping was restrained along the entire length. Fig. 2 illustrates the general model layout.

2.2 Model Verification

While ABAQUS (Dassault Systèmes, SIMULIA, 2023) provides a highly detailed platform for nonlinear analysis, its complexity results in high computational time and storage requirements.

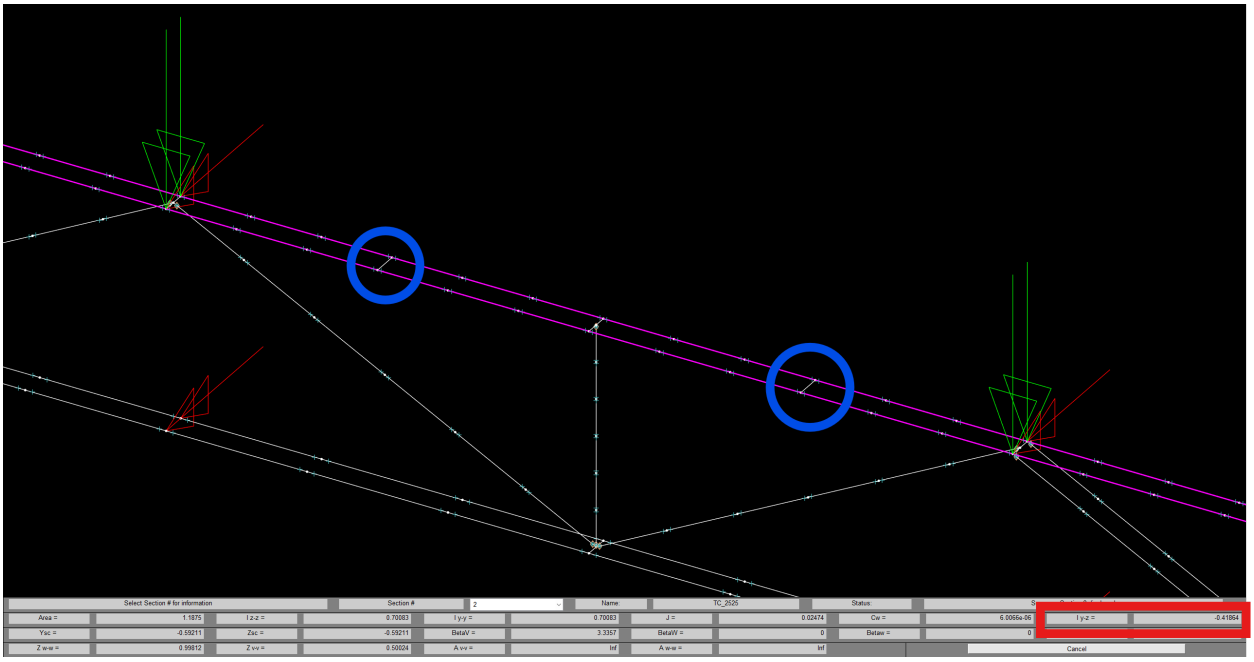

Figure 1: MASTAN2 model showing fillers (blue circles) and product moment of inertia (red) in advanced section properties definitions

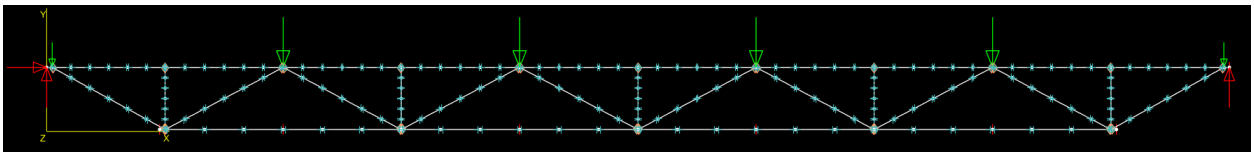

Figure 2: Generic layout of one modeled girder (SJI1A) in MASTAN2

Therefore, MASTAN2 (Ziemian, McGuire, and Liu, 2019) was selected for this parametric study because it offers high accuracy with significantly lower computational time and storage demands.

To verify the modeling approach used in MASTAN2, a representative joist girder model, SJI1A, was also modeled in ABAQUS for comparison. To ensure consistency, both models shared identical geometry, boundary conditions, applied load, and material properties and definitions, including the use of plastic hinge theory. Second-order analyses were performed in both software platforms.

As shown in Fig. 3, the relationship between the Load Proportional Factor (LPF) and vertical displacement at mid span shows a match between the two software analysis results. This comparison confirms that the load path and general structural behavior modeled in MASTAN2 are consistent with those obtained from a more detailed finite element model in ABAQUS.

2.3 Buckling Analysis

Due to variations in lateral bracing lengths and member sizes, both elastic and inelastic 3D buckling analyses were employed throughout the study. Figs. 4 and 5 show examples of buckled top chord members in the 3D eigenbuckling analysis with different global flexural buckling shapes depending on the varying unbraced length.

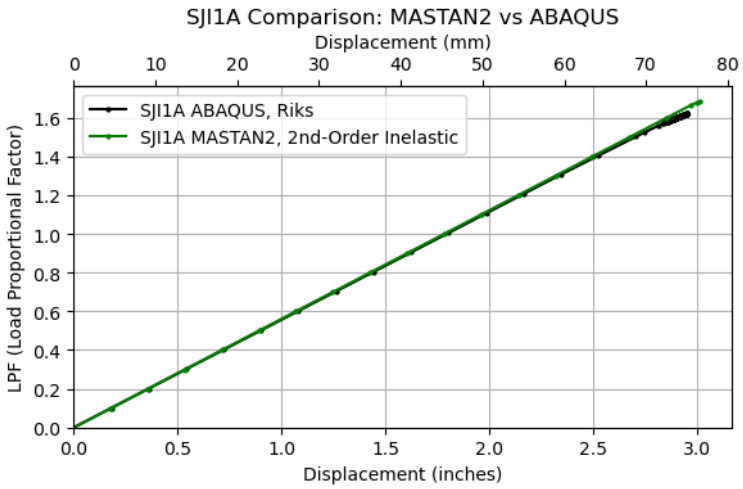

Figure 3: The comparison of MASTAN2 and ABAQUS for model validation

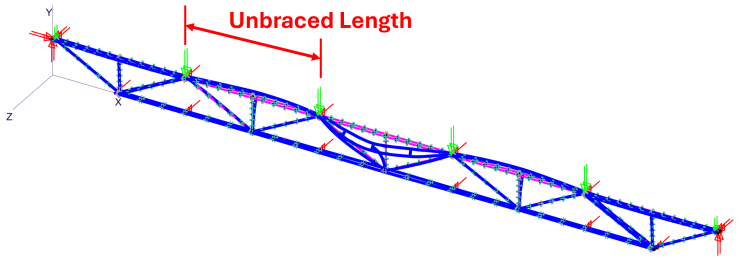

Figure 4: Buckled shape for the original unbraced length in MASTAN2 (deflected shape scaled by a factor of 15)

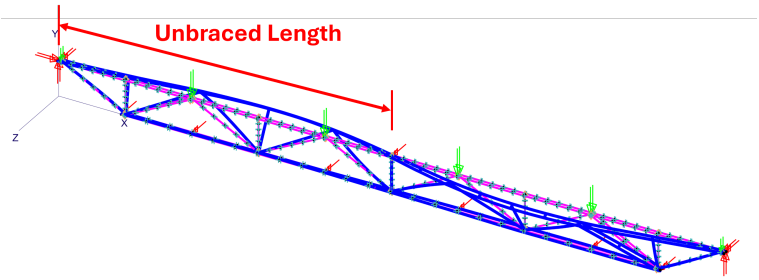

Figure 5: Buckled shape for the changed unbraced length in MASTAN2 (deflected shape scaled by a factor of 15)

MASTAN2 supports both basic and advanced section properties. The advanced section property include the product moment of inertia as an input parameter, which is related to the least radius of gyration r_z. As a result, the advanced section property can capture the principal-axis behavior, whereas the basic section property cannot because it does not account for the product moment of inertia. To evaluate the impact of the modified slenderness ratio, models were analyzed with and without r_z. Additionally, filler elements were used to simulate the effect of l_s on the buckling capacity of the top chords. Fig. 1 illustrates a model using advanced properties with filler elements highlighted in blue circles and the product moment of inertia in red.

3. Calculation Process for Slenderness Ratio and Critical Stress

The critical stress, F_{cr}, is calculated by considering the slenderness ratio according to AISC 360-10 formulations as follows:

$$\textbf{Slenderness Ratio} = \frac{k\ell}{r} \begin{cases} \frac{k\ell}{r} \leq 4.71\sqrt{\frac{E}{QF_y}} \xrightarrow{\textbf{Inelastic Region}} \mathbf{F_{cr}} = Q\left[0.658^{\left(\frac{QF_y}{F_e}\right)}\right]F_y \\ \frac{k\ell}{r} > 4.71\sqrt{\frac{E}{QF_y}} \xrightarrow{\textbf{Elastic Region}} \mathbf{F_{cr}} = 0.877F_e \end{cases}$$

where k is the effective length factor, ℓ is the member length, and r is the radius of gyration, Q is the full reduction factor for slender compression members which will be discussed in the next section, F_y is the yield stress of the material.

The MASTAN2 buckling analysis calculates the buckling load for the system and provides the forces in each element. Therefore, the forces in the top chord at the buckling load were used to calculate the resulting member slenderness (Kim, Sputo, and Blum, 2024). The relationship between slenderness ratio and critical stress values (F_{cr}) provided in AISC 360-10 (AISC 360-10, 2010) and SJI 100-2020 Standard (Steel Joist Institute, 2020) were used. The slenderness calculation procedure is completed as follows:

$$F_{cr} = \frac{F}{A} \begin{cases} \text{Back-calculated slenderness ratio (Inelastic)} = \sqrt{\left(\frac{\pi^2 E}{Q \cdot F_y}\right) \cdot \left(\log_{0.658}\left(\frac{F_{cr}}{Q \cdot F_y}\right)\right)} \\ \text{Back-calculated slenderness ratio (Elastic)} = \sqrt{0.877 \cdot \frac{\pi^2 E}{F_{cr}}} \end{cases}$$

where F is the axial force corresponding to the buckling failure load obtained from MASTAN2, and A is the cross-sectional area of the top chord section. A comparison was then made between the slenderness ratio obtained from the analysis results and the values calculated using standard design equations. In addition to the slenderness ratio, the critical stress F_{cr} values were also compared between the model output and Standard predictions.

A schematic overview of the entire slenderness calculation process is presented below.

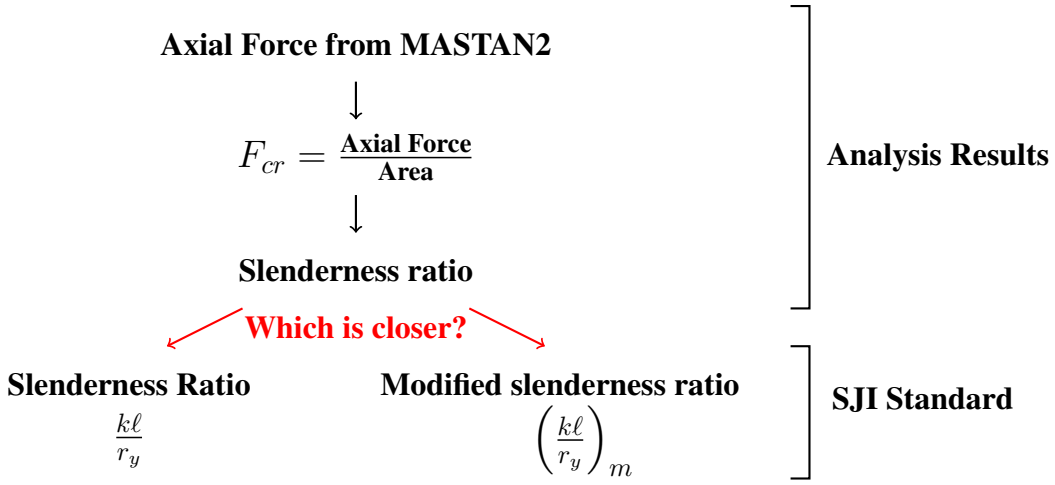

To evaluate their specific impacts, the individual and combined effects of r_z (cross-sectional) and l_s (fillers) were also analyzed. The modified slenderness ratio, which accounts for both parameters, is presented alongside corresponding F_{cr} values in Sections 4.2 and 4.3 for comparison.

4. Results and Discussion

This section presents the results by comparing the slenderness ratio and critical stress (F_{cr}) values obtained from structural analyses with those calculated using the formulas recommended in current design standards (AISC 360-10, 2010 and Steel Joist Institute, 2020).

4.1 Full Reduction Factor, Q for Slender Compression Members

In the evaluation of compressive strength for slender steel members, a reduction factor, Q, is applied to account for local buckling effects in slender elements. This factor is particularly relevant for members such as double-angle joist girder top chords, which may contain slender unstiffened elements. Consistent with current design standards (AISC 360-10, 2010 and Steel Joist Institute, 2020), the reduction factor modifies the yield stress used in determining the critical buckling stress, F_{cr}.

The reduction factor Q is defined as the product of two components as shown in Eq. 2:

$$Q = Q_s Q_a \tag{2}$$

where Q_s represents the reduction factor for slender unstiffened elements and Q_a corresponds to slender stiffened elements. Since the compression chord members examined in this study consist of double-angle sections without stiffened plate elements, only Q_s is applicable, and Q_a is taken as 1.0.

The value of Q_s is determined based on the width-to-thickness ratio of the angle legs, following the expressions provided in the AISC and SJI specifications. Depending on the cross-sectional proportions, Q_s may be equal to unity for compact elements or less than unity for increasingly slender elements. For the chord sections considered in this study, Q_s values slightly below unity

were obtained for the larger angle sizes.

The inclusion of Q introduces an upper bound on the critical stress in the inelastic buckling formulation, as shown in Eq. 3:

$$F_{cr} \leq QF_y \tag{3}$$

As a result, when calculated F_{cr} values obtained from finite element analysis exceed this limit, the corresponding inelastic slenderness ratios cannot be evaluated using the logarithmic formulation prescribed by the specification. These cases are therefore excluded from further comparison in the subsequent results.

4.2 Slenderness Ratios and F_{cr} Values from Analyses Results

Slenderness ratios and F_{cr} values were determined using the slenderness calculation method described in Section 3. Tables 1, 2, and 3 present these results and indicate whether buckling occurs in the elastic or inelastic region. Any calculated values that do not satisfy the condition in Equation 3 are excluded from further interpretation in this study.

The effect of the least radius of gyration (r_z) is observed by comparing F_{cr} and slenderness ratios between Basic and Advanced sections in the same row in the Tables. Similarly, the influence of filler elements (l_s) is shown by the differences between the original unbraced lengths (the first two rows) and the modified unbraced lengths (the third and the fourth rows) for each model.

4.2.1 Comparison of Slenderness Ratios

Slenderness ratios that were obtained using the MASTAN2 results (the fifth and the seventh columns) and slenderness ratios that were calculated with the SJI standard (the columns from eight to eleven) are presented in Tables 1, 2, and 3. Additional comparison plots between the slenderness ratios calculated from the MASTAN2 buckling results and standard slenderness ratios are also shown in Figs. 6, 7, and 8.

4.2.2 Comparison of Critical Stress Values, F_{cr}

Calculated critical stress values determined from the buckling analysis results and critical stress values calculated from the slenderness and modified slenderness formulas in the Specification were also compared in Figs. 9, 10, and 11.

4.3 Discussion

Tables 1, 2, and 3 show that the influence of the least radius of gyration (r_z) increases from member A to D. This is expected, as larger cross-sections have higher r_z values, which improve weak-axis bending stiffness and buckling resistance. Similarly, the effect of fillers (l_s) is more significant in members with lower slenderness ratios. By delaying local buckling, fillers help postpone global flexural buckling, a finding that aligns with Sippel et al. (2022).

However, Figs. 9–8 indicate that using the modified slenderness ratio is generally unnecessary for these members. The results suggest that the commonly assumed effective length factor (k) of 0.94

Table 1: Back-calculated F_{cr} and Slenderness ratio values from MASTAN2 and the SJI standard slenderness ratios for girder group 1

			Back-Calculated by Analysis				**Calculated by Standard Formulas**			
SJI1A			**Basic Section**		**Adv. Sect.**		**SJI Slenderness**		**Mod. Slend.**	
L (inch)	l_s (inch)	Category	F_{cr}	Slend. Rat.	F_{cr}	Slend. Rat.	k = 0.94	k = 1	k = 0.94	k = 1
86.38	43.25	Inelastic	41520.84	50.41	40086.74	54.97	53.50	56.91	69.27	71.94
86.38	21.63	Inelastic	45696.84	35.08	44922.11	38.27	53.50	56.91	57.84	61.02
216.0	43.25	Elastic	27627.79	95.32	23363.37	103.65	133.78	142.32	140.83	148.96
216.0	21.63	Elastic	30750.32	90.35	25477.05	99.26	133.78	142.32	135.58	144.01

SJI1B			**Basic Section**		**Adv. Sect.**		**SJI Slenderness**		**Mod. Slend.**	
L (inch)	l_s (inch)	Category	F_{cr}	Slend. Rat.	F_{cr}	Slend. Rat.	k = 0.94	k = 1	k = 0.94	k = 1
86.38	43.25	Inelastic	46999.78	29.09	46114.97	33.26	53.50	56.91	69.27	71.94
86.38	21.63	Inelastic	48489.62	20.48	47961.51	23.86	53.50	56.91	57.84	61.02
216.0	43.25	Inelastic	43488.52	43.68	40540.33	53.56	133.78	142.32	140.83	148.96
216.0	21.63	Inelastic	44744.04	38.97	41823.83	49.42	133.78	142.32	135.58	144.01

SJI1C			**Basic Section**		**Adv. Sect.**		**SJI Slenderness**		**Mod. Slend.**	
L (inch)	l_s (inch)	Category	F_{cr}	Slend. Rat.	F_{cr}	Slend. Rat.	k = 0.94	k = 1	k = 0.94	k = 1
86.38	43.25	Inelastic	48138.13	15.63	47412.27	21.36	53.50	56.91	69.27	71.94
86.38	21.63	Inelastic	49050.23	N/A	48670.58	9.52	53.50	56.91	57.84	61.02
216.0	43.25	Inelastic	46493.02	27.01	44621.07	36.10	133.78	142.32	140.83	148.96
216.0	21.63	Inelastic	47309.60	22.06	46122.92	29.00	133.78	142.32	135.58	144.01

SJI1D			**Basic Section**		**Adv. Sect.**		**SJI Slenderness**		**Mod. Slend.**	
L (inch)	l_s (inch)	Category	F_{cr}	Slend. Rat.	F_{cr}	Slend. Rat.	k = 0.94	k = 1	k = 0.94	k = 1
86.38	43.25	Inelastic	48744.35	N/A	40086.74	N/A	53.50	56.91	69.27	71.94
86.38	21.63	Inelastic	49339.13	N/A	44922.11	N/A	53.50	56.91	57.84	61.02
216.0	43.25	Inelastic	41182.61	N/A	23363.37	15.07	133.78	142.32	140.83	148.96
216.0	21.63	Inelastic	48549.57	N/A	25477.05	9.33	133.78	142.32	135.58	144.01

Table 2: Back-calculated F_{cr} and Slenderness ratio values from MASTAN2 and the SJI standard slenderness ratios for girder group 2

SJI2A			**Basic Section**		**Adv. Sect.**		**SJI Slenderness**		**Mod. Slend.**	
L (inch)	l_s (inch)	Category	F_{cr}	Slend. Rat.	F_{cr}	Slend. Rat.	k = 0.94	k = 1	k = 0.94	k = 1
115.13	57.63	Inelastic	34147.37	72.22	32236.74	77.23	71.30	75.85	92.31	95.87
115.13	28.81	Inelastic	41335.58	51.02	40040.42	55.12	71.30	75.85	77.09	81.32
288.00	57.63	Elastic	16832.84	122.12	15344.00	127.90	178.37	189.76	187.76	198.61
288.00	28.81	Elastic	18937.26	115.13	16982.74	121.58	178.37	189.76	180.76	192.01

SJI2B			**Basic Section**		**Adv. Sect.**		**SJI Slenderness**		**Mod. Slend.**	
L (inch)	l_s (inch)	Category	F_{cr}	Slend. Rat.	F_{cr}	Slend. Rat.	k = 0.94	k = 1	k = 0.94	k = 1
115.13	57.63	Inelastic	44048.09	41.63	42775.08	46.20	50.48	53.70	62.34	64.98
115.13	28.81	Inelastic	46821.42	31.21	45593.88	35.52	50.48	53.70	53.69	56.73
288.00	57.63	Elastic	33438.08	86.64	28032.35	94.63	126.29	134.35	131.48	139.24
288.00	28.81	Elastic	35616.17	83.95	29319.69	92.53	126.29	134.35	127.60	135.59

SJI2C			**Basic Section**		**Adv. Sect.**		**SJI Slenderness**		**Mod. Slend.**	
L (inch)	l_s (inch)	Category	F_{cr}	Slend. Rat.	F_{cr}	Slend. Rat.	k = 0.94	k = 1	k = 0.94	k = 1
115.13	57.63	Inelastic	46392.73	27.56	45392.29	32.62	42.27	44.97	51.39	53.63
115.13	28.81	Inelastic	48002.03	16.85	47352.58	21.77	42.27	44.97	44.72	47.28
288.00	57.63	Inelastic	41529.02	48.02	37797.06	60.17	105.75	112.50	109.71	116.23
288.00	28.81	Inelastic	42584.37	44.22	38852.42	56.88	105.75	112.50	106.75	113.44

SJI2D			**Basic Section**		**Adv. Sect.**		**SJI Slenderness**		**Mod. Slend.**	
L (inch)	l_s (inch)	Category	F_{cr}	Slend. Rat.	F_{cr}	Slend. Rat.	k = 0.94	k = 1	k = 0.94	k = 1
115.13	57.63	Inelastic	47596.52	11.81	46720.00	20.10	36.33	38.65	43.72	45.67
115.13	28.81	Inelastic	48702.61	N/A	48240.00	N/A	36.33	38.65	38.31	40.52
288.00	57.63	Inelastic	44963.48	30.81	42504.35	41.83	90.89	96.69	94.09	99.71
288.00	28.81	Inelastic	45996.52	25.02	43678.26	36.90	90.89	96.69	91.70	97.46

Table 3: Back-calculated F_{cr} and Slenderness ratio values from MASTAN2 and the SJI standard slenderness ratios for girder group 3

SJI3A			**Basic Section**		**Adv. Sect.**		**SJI Slenderness**		**Mod. Slend.**	
L (inch)	l_s (inch)	Category	F_{cr}	Slend. Rat.	F_{cr}	Slend. Rat.	k = 0.94	k = 1	k = 0.94	k = 1
102.88	51.50	Inelastic	36610.53	65.29	35227.79	69.21	63.71	67.78	82.49	85.67
102.88	25.75	Inelastic	42236.63	48.04	41226.95	51.37	63.71	67.78	68.89	72.67
360.00	51.50	Elastic	12064.00	144.25	10974.32	151.24	222.96	237.20	229.04	242.91
360.00	25.75	Elastic	13030.74	138.79	11679.16	146.60	222.96	237.20	224.50	238.64

SJI3B			**Basic Section**		**Adv. Sect.**		**SJI Slenderness**		**Mod. Slend.**	
L (inch)	l_s (inch)	Category	F_{cr}	Slend. Rat.	F_{cr}	Slend. Rat.	k = 0.94	k = 1	k = 0.94	k = 1
102.88	51.50	Inelastic	44971.37	38.07	44002.62	41.80	45.11	47.99	55.71	58.07
102.88	25.75	Inelastic	46667.54	30.71	45838.69	34.47	45.11	47.99	47.98	50.70
360.00	51.50	Elastic	23736.31	102.84	19973.60	112.10	157.86	167.93	161.21	171.09
360.00	25.75	Elastic	24591.39	101.03	20363.89	111.02	157.86	167.93	157.70	168.73

SJI3C			**Basic Section**		**Adv. Sect.**		**SJI Slenderness**		**Mod. Slend.**	
L (inch)	l_s (inch)	Category	F_{cr}	Slend. Rat.	F_{cr}	Slend. Rat.	k = 0.94	k = 1	k = 0.94	k = 1
102.88	51.50	Inelastic	46944.29	24.39	46120.54	29.02	37.77	40.18	45.92	47.92
102.88	25.75	Inelastic	48307.66	13.97	47789.53	18.59	37.77	40.18	39.97	42.25
360.00	51.50	Elastic	35643.37	83.92	29418.67	92.37	132.18	140.62	134.74	143.03
360.00	25.75	Elastic	38002.40	81.27	30662.66	90.48	132.18	140.62	132.83	141.23

SJI3D			**Basic Section**		**Adv. Sect.**		**SJI Slenderness**		**Mod. Slend.**	
L (inch)	l_s (inch)	Category	F_{cr}	Slend. Rat.	F_{cr}	Slend. Rat.	k = 0.94	k = 1	k = 0.94	k = 1
102.88	51.50	Inelastic	47984.35	4.91	47313.04	14.98	32.47	34.54	39.07	40.81
102.88	25.75	Inelastic	48895.65	N/A	48483.48	N/A	32.47	34.54	34.24	36.21
360.00	51.50	Inelastic	40544.35	49.20	35991.30	64.15	113.62	120.87	115.68	122.81
360.00	25.75	Inelastic	41686.96	45.01	36925.22	61.25	113.62	120.87	114.13	121.36

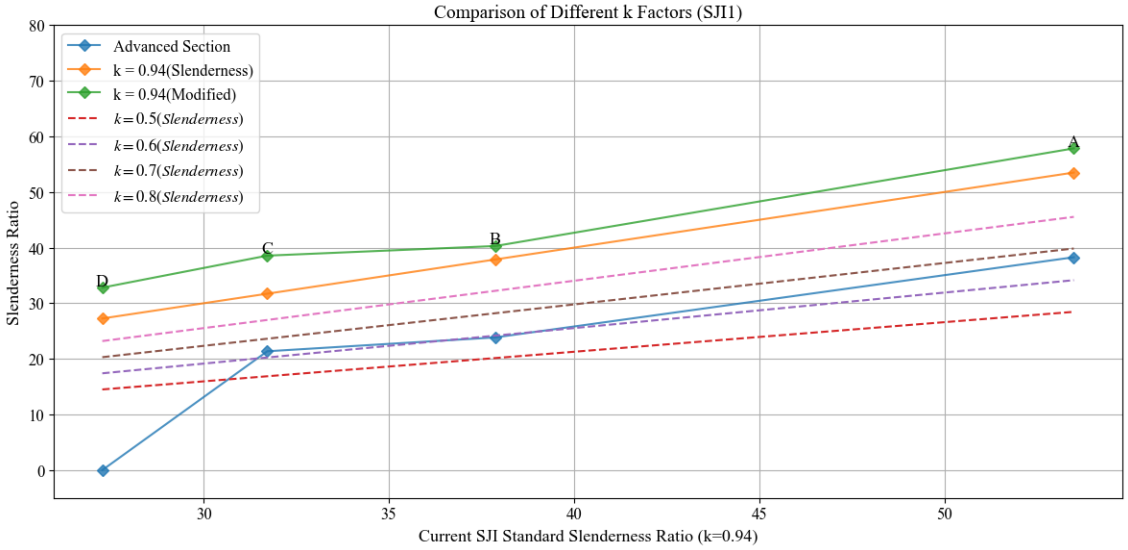

Figure 6: The comparison of slenderness ratios with suggested effective length factors for SJI1

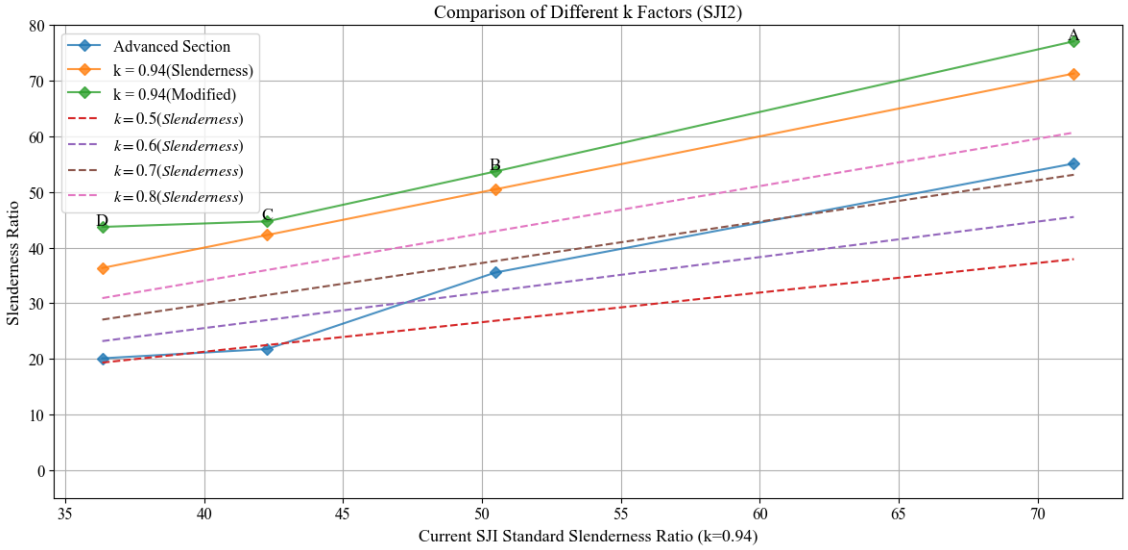

Figure 7: The comparison of slenderness ratios with suggested effective length factors for SJI2

is overly conservative. To investigate potential improvements in structural efficiency, slenderness ratios were recalculated using lower k values (0.5, 0.6, 0.7 and 0.8) and compared against calculated slenderness values from MASTAN2 buckling results and Specification equations. Based on the plots, $k = 0.8$ may be an efficient solution while still maintaining sufficient design conservatism. Future research is recommended to determine an appropriate k factor for joist girder chord members.

5. Conclusion

This study evaluated the compressive behavior of steel joist girder chord members through a parametric analysis. Three distinct joist girder designs were modeled in MASTAN2, resulting in 96

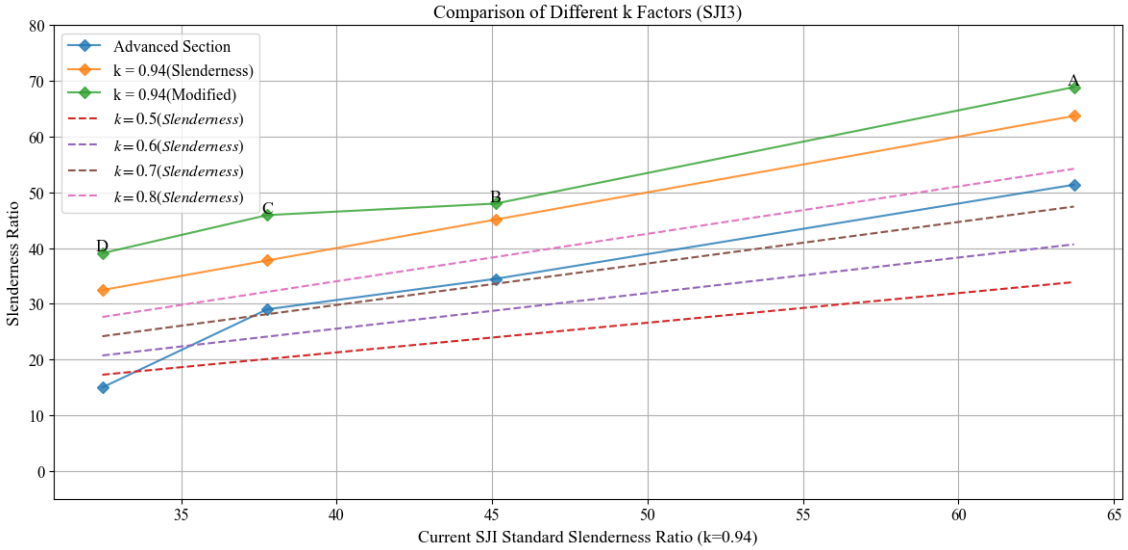

Figure 8: The comparison of slenderness ratios with suggested effective length factors for SJI3

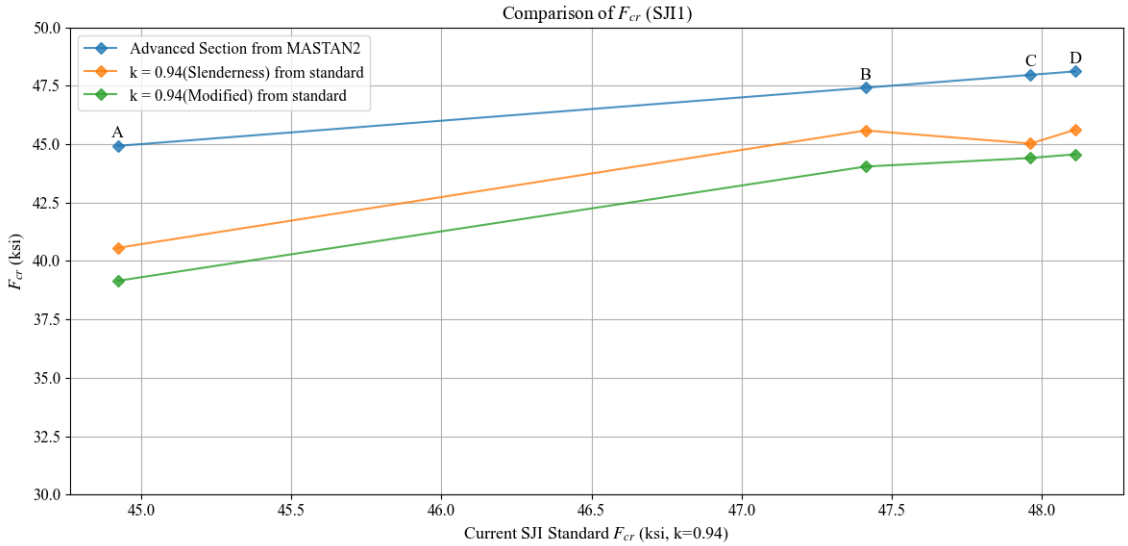

Figure 9: The comparison of F_{cr} for SJI1

different configurations that accounted for variations in cross-sections, unbraced lengths, and filler element placement. Using eigenvalue buckling analysis, the critical buckling capacities were determined and used to calculate equivalent slenderness ratios. These results were then compared with the slenderness ratios predicted by SJI and AISC Specification formulas to evaluate the necessity of the modified slenderness ratio in current design practices.

The findings indicate that while the least radius of gyration (r_z) and filler spacing (l_s) influence structural stability, current Specification equations tend to overestimate the actual slenderness of the system. Specifically, the results show that incorporating the modified slenderness ratio leads to overly conservative designs for these compression members. This trend is clearly supported by the back-calculated critical stress (F_{cr}) values from the buckling analysis results, which remained

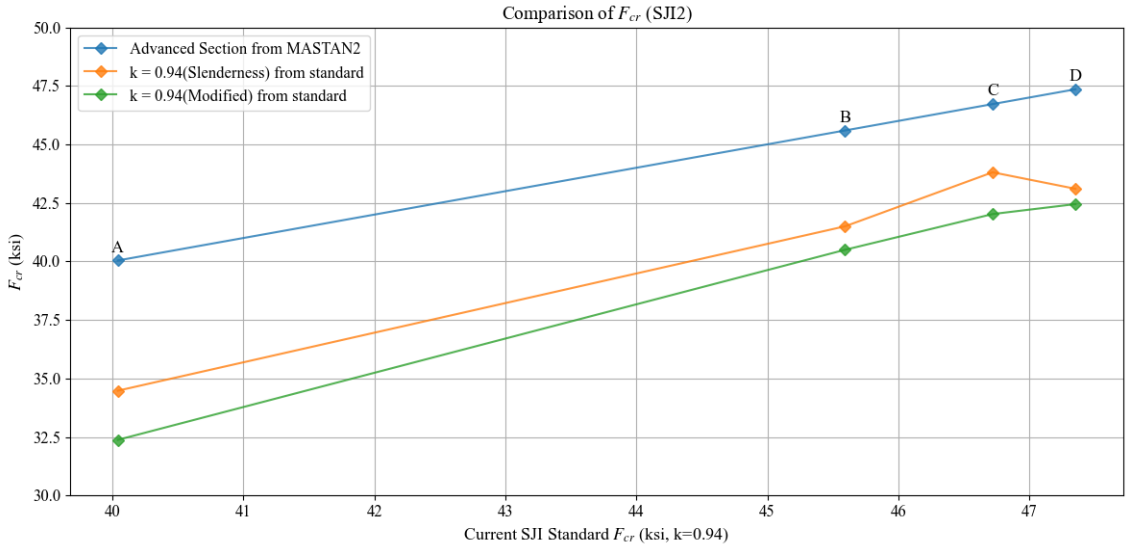

Figure 10: The comparison of F_{cr} for SJI2

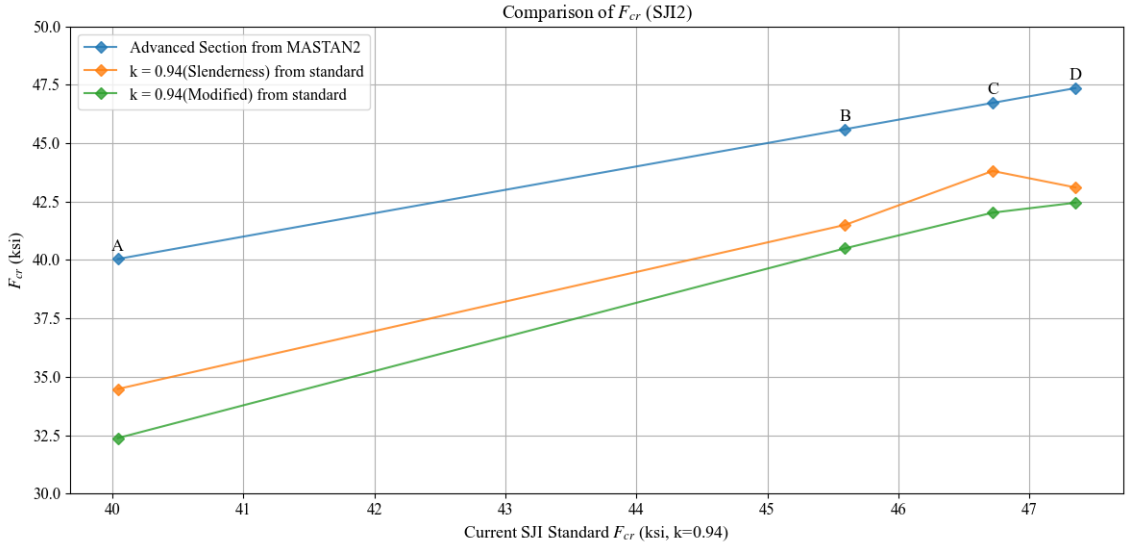

Figure 11: The comparison of F_{cr} for SJI3

consistently higher than the strengths predicted by the Specification equations. These results suggest that for the joist girder configurations studied, the additional safety margin provided by the modified slenderness ratio may be unnecessary and could be reduced to improve design efficiency without compromising safety.

Acknowledgments

The authors would like to thank the Steel Joist Institute (SJI) for supporting the project through a research grant.

References

AISC 360-10 (2010). *Specification for Structural Steel Buildings*. ANSI/AISC.

Cicek, Kubilay, Thomas Sputo, and Hannah B Blum (2024). "The impact of analysis assumptions on buckling prediction in open-web steel joists". *Annual Stability Conference, Structural Stability Research Council*.

Dassault Systèmes, SIMULIA (2023). *Abaqus 2023*. Dassault Systèmes.

Kim, Useok, Kubilay Cicek, and Hannah B. Blum (Aug. 2025). *Modified Slenderness Ratio of Joist Girder Chord Members*. Technical Report. Florence, SC: Steel Joist Institute.

Kim, Useok, Thomas Sputo, and Hannah B. Blum (May 2024). *Modified Slenderness Ratio of Joist Chord Members*. Technical Report. Florence, SC: Steel Joist Institute.

Sippel, Edward J, Ronald D Ziemian, and Hannah B Blum (2022). "Influence of torsional stiffness in double-angle open-web joist and joist girder chords". *Journal of Constructional Steel Research* 199, p. 107595.

Sippel, Edward J et al. (2020). *Tutorial for MASTAN2 v5.1 - Steel Joist*. https://www.mastan2.com/data/Joist_Tutorial.pdf.

Steel Joist Institute (2020). *ANSI/SJI 100 – 2020, Standard Specification for K-Series, LH-Series, and DLH-Series Open Web Steel Joists, and for Joist Girders*. Florence, SC, U.S.A.

Ziemian, R. D., W. McGuire, and S. W. Liu (2019). *MASTAN2*.